Z. Kristallogr. Suppl. **26** (2007) 455-460

Combined high resolution powder and single-crystal diffraction to determine the structure of $Li_{1+x}Ce^{III}_{x}Ce^{IV}_{6-x}F_{25}$

G. Renaudin[1*], E. Mapemba[1], M. El-Ghozzi[1], M. Dubois[1], D. Avignant[1], R. Černý[2]

[1] Université Blaise Pascal, Laboratoire des Matériaux Inorganiques, UMR 6002 CNRS, 24 Avenue des Landais, F-63177 Aubière, France.
[2] University of Geneva, Laboratory of Crystallography, 24 quai Ernest-Ansermet, CH-1211 Geneva 4, Switzerland.
[*] Contact author; e-mail: guillaume.renaudin@ensccf.fr

Keywords: powder diffraction, single-crystal diffraction, lattice symmetry, mixed valence cerium fluoride

Abstract. The $Li_{1+x}Ce_6F_{25}$ compound is a mixed valence cerium fluoride. Moderate temperature solid state synthesis has been used to grow single-crystals. Single- crystal X-ray diffraction intensities data were collected at room temperature using a Stoe IPDS II image plate diffractometer. The structure was first solved and refined in the $P4_1$ space group (a = 8.855 (2) Å and c = 22.968 (5) Å) from the single-crystal X-ray data but a high resolution synchrotron powder diffraction experiment performed on a powdered sample at the Swiss-Norvegian Beam Line (SNBL) at ESRF, Grenoble, showed the true symmetry to be monoclinic. The powder pattern revealed a weak splitting of numerous peaks due to a lowering of the lattice symmetry. The pattern was successfully indexed with a monoclinic cell (a = 8.82391 (7) Å, b = 22.9188 (2) Å, c = 8.85384 (7) Å and β = 90.6093 (2)°) corresponding to a weak distortion of the tetragonal cell previously observed from single-crystal. The definitive structure was refined in the monoclinic $P2_1$ space group using single-crystal intensities data combined with the lattice refined from synchrotron powder pattern. The main structural characteristics are identical in both models; either in the average tetragonal $P4_1$ model or in the correct monoclinic $P2_1$ one and revealed a long-range ordering between trivalent and tetravalent cerium cations (by the way of valence calculation). The lithium ions are divided into two groups, the first ones being susceptible to move in the opened channels of the structure, the others being locked in the slabs of this structure.

Introduction

Because of their potential applications related to the electronic exchange and magnetism, compounds exhibiting mixed-valence are the subject of numerous investigations. In this framework, the crystal-chemical properties of tetravalent terbium fluorides have extensively been studied because the half-filled shell of the $4f^7$ electronic configuration of the tetravalent

terbium stabilizes the IV oxidation state and also because the thermal decomposition of the terbium tetrafluoride, even under fluorine atmosphere, at moderate temperature allows the formation of mixed-valence compounds. The presence of alkaline ions also favors the mixed-valence formation. Before this study no mixed-valence cerium fluoride has been reported in the literature. Since the crystal-chemistry of both terbium and cerium fluorides exhibit some similarities, this work was carried out with the aim to stabilize and characterize new mixed-valence cerium fluorides. The synthesis and the crystal chemistry of the title compound will be fully described elsewhere [1]. The structure consists of a three-dimensional framework of 8- and 9-fluorine coordinated cerium polyhedra linked by edge and corner-sharing. Some cerium atoms exhibit mixed III/IV valence. From valence calculation a long-range ordering between the Ce^{3+} and Ce^{4+} cations has been evidenced. The three-dimensional structure may be regarded as a stacking along the two-fold axis of two kinds of slabs. The first ones are opened slabs built of 8-coordinated mixed valence III/IV Ce. The second ones are locked slabs built of 8- and 9-coordinated tetravalent Ce (see figure 1). The existence of two different environments for the Li^+ cations was confirmed by ^{7}Li MAS NMR experiment [1]. The aim of the present paper is to show how the contribution of high resolution powder diffraction has allowed the true lattice symmetry and space group to be determined. Whereas single-crystal diffraction data indicated a tetragonal lattice (a = 8.855 (2) Å, c = 22.968 (5) Å), synchrotron powder pattern clearly shows a splitting of numerous diffraction peaks (see figure 2) disclosing a weak monoclinic distortion of the lattice (a = 8.82391 (7) Å, b = 22.9188 (2) Å, c = 8.85384 (7) Å, β = 90.6093 (2)°). The crystal structure was solved in the tetragonal symmetry ($P4_1$ space group) but should be better described in the lower monoclinic ones ($P2_1$ space group). This paper gives also a comparison between the two refined models.

Experimental and results

Synthesis

Samples, used for single-crystal and synchrotron powder measurements, were prepared by solid state reaction involving mixtures of LiF, CeF_3 and CeF_4 starting materials in the ratio 1/1/3. The mixtures were introduced in a platinum tubes further sealed under dry argon atmosphere and heated at 823 K for 12 hours. Orange single-crystals were isolated from a batch.

Single crystal X-rays diffraction

Single-crystal X-ray diffraction intensities data were collected at room temperature with a Stoe IPDS II image plate diffractometer. The observed reciprocal lattice indicated a tetragonal lattice with a = 8.855 (2) Å and c = 22.968(5) Å. The structure was solved with *SHELXS97* [2] and refined with *SHELXL97* [3] programs in the $P4_1$ space group (R_{int} = 0.054, R_F = 0.080, R_{wF} = 0.151 and s = 1.39 for 165 parameters refined from 4583 unique reflections). More details are given in [1].

Synchrotron high resolution powder diffraction

Synchrotron powder diffraction data of a freshly synthesized sample was performed at the Swiss-Norwegian Beam Line (SNBL) at the ESRF in Grenoble (sample in a 0.2 mm glass capillary, six-analyzer crystals detector, wavelength of 0.37504 Å, two theta range from 1.0° to 17.5° and two theta step of 0.002°). Synchrotron powder diffraction data were used to

check the symmetry of the compound with *FullProf.2k* [4]. A weak monoclinic lattice distortion corresponding to the unit cell a = 8.82391 (7) Å, b = 22.9188 (2) Å, c = 8.85384 (7) Å, β = 90.6093 (2)° was observed. Figure 2 displays the peaks splits due to the lowering of the symmetry. The structure was then refined in the $P2_1$ space group (328 parameters refined from 8776 unique reflections with R_{int} = 0.053, R_F = 0.075, R_{wF} = 0.142 and s = 1.11) using intensities data from single crystal measurement transformed in the monoclinic setting deduced from synchrotron powder pattern. More details are given in [1].

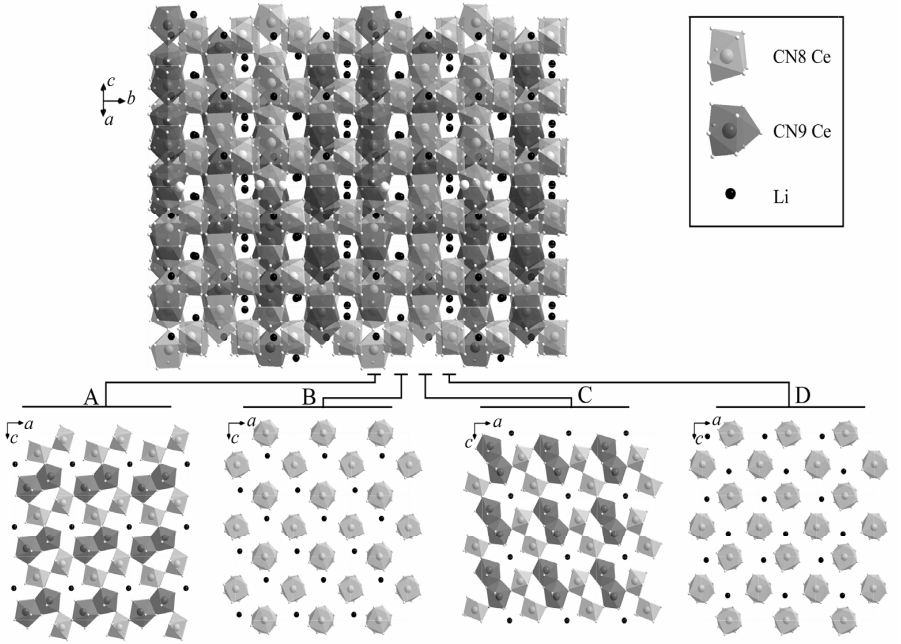

Figure 1. General representation along [101] and four details (A, B, C and D) along [010] of the $Li_{1+x}Ce_6F_{25}$ monoclinic $P2_1$ structure. Small white, large light grey, dark grey and black balls correspond to fluorine, CN8 cerium, CN9 cerium and lithium atoms respectively.

Discussion and conclusions

Each atomic position of the average tetragonal $P4_1$ model (the unique Wyckoff position of this group is 4*a*) splits into two independent crystallographic sites 2*a* in the $P2_1$ subgroup. The tetragonal $P4_1$ description of the structure includes 6 cerium, 25 fluorine and 3 lithium independent sites (a total of 34 independent sites). The corresponding 68 atomic sites of the monoclinic $P2_1$ description [1] correlated two by two by a pseudo four-fold screw axis can be merged in a quasi-equivalent tetragonal model. The 34 refined atomic positions of the tetragonal $P4_1$ model (labelled in *italic* in this paper) are gathered with the corresponding 68 independent atomic positions of the monoclinic description [1] in tables 1 (for Ce sites) and 2 (for F and Li sites). The atomic positions refined in the monoclinic lattice have been

transformed into the pseudo-equivalent tetragonal lattice to allow the comparison between the two models (columns labelled 'atomic shift $P4_1$-$P2_1$' in tables) and to estimate the deviation from the pseudo four-fold screw axis in the $P2_1$ model (columns labelled 'atomic shift $P2_1$-$P2_1$' in tables). The obtained atomic shifts illustrate the great similitude between the average $P4_1$ model and the true $P2_1$ one. In the same way, the calculated shift between atomic positions linked two by two by the pseudo four-fold screw axis in the $P2_1$ model gives another evidence of this great similitude.

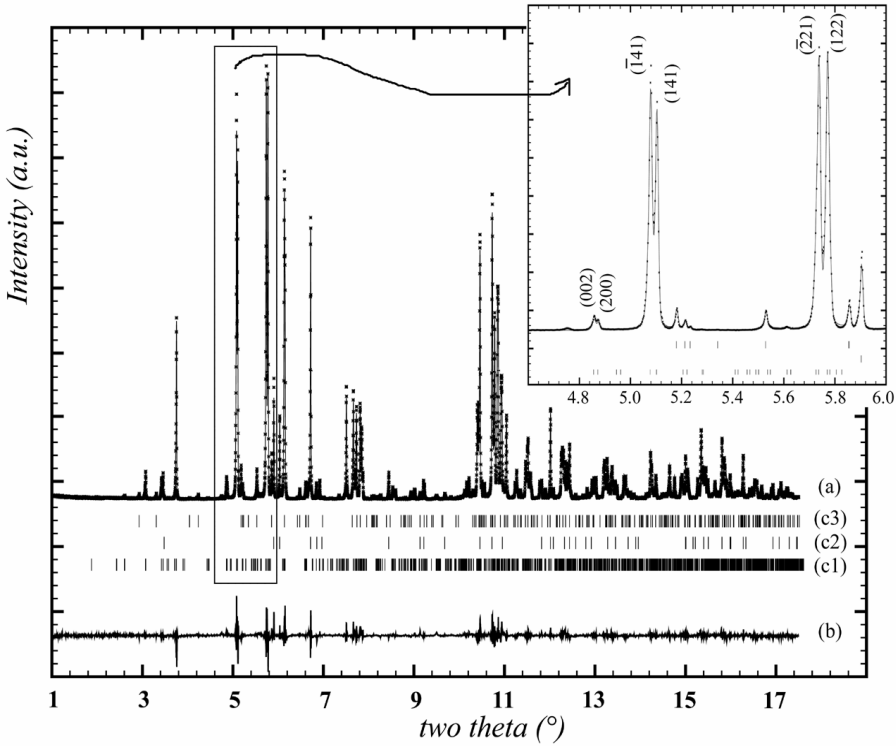

Figure 2. Rietveld plot of $Li_{1+x}Ce_6F_{25}$. Observed (a: dots) and calculated (a: solid line) synchrotron (SNBL) powder diffraction pattern (λ = 0.37504 Å) are shown with difference curve (b) and Bragg peak positions for $Li_{1+x}Ce_6F_{25}$ (c1) and impurities CeF_3 (c2) and CeF_4 (c3). Splitting due to the monoclinic distortion of the lattice is illustrated in the insert.

Both $P4_1$ and $P2_1$ models give the same array of 8- and 9-coordinated cerium atoms shown in figure 1. Bond valence calculation led to the same long-range order between Ce^{3+} and Ce^{4+} cations; opened slabs are composed by 8-coordinated mixed valence Ce^{3+}/Ce^{4+}, and locked slabs are composed by half 8- and half 9-coordinated Ce^{4+}. The only difference comes from the long-range ordering between Ce^{3+} and Ce^{4+} in the opened slabs. Although the model refined in the $P4_1$ space group conserved a long-range ordering of cerium mixed valence in open slabs, a translation of $\frac{1}{2}(\vec{a}+\vec{b})$ is observed as shown in table 1 by the calculated

valence for *Ce1* and *Ce2* (inverted in comparison with equivalent positions in the $P2_1$ model). The obtained value for the *Ce1* bond valence results from the shifts of the positions of the eight coordinated fluorines *F18*, *F25*, *F7*, *F17*, *F6*, *F10*, *F8* and *F16* which can reach an average value of 0.22 Å from those generated by the pseudo tetragonal screw axis compared to the other values less than 0.08 Å (table 2). The value of the *Ce2* valence can be explained by the important atomic shift (0.05 Å) from the positions given by the pseudo tetragonal screw axis (table 1, compared to the other values less than 0.02 Å). The existence of a long-range ordering between Ce^{3+} and Ce^{4+} seems to be responsible of the loss of the tetragonal screw axis leading to the monoclinic symmetry.

Table 1. Comparison of the cerium environment between the average $P4_1$ model and the correct $P2_1$ one (transformed in the tetragonal symmetry). Atom labels used for the $P2_1$ model correspond to [1].

Atom label in		Atomic shift (Å)		Polyhedron volume (Å^3)		Bond valence				Valence	
						$P4_1$		$P2_1$			
$P4_1$	$P2_1$	$P4_1$-$P2_1$	$P2_1$-$P2_1$	$P4_1$	$P2_1$	Ce^{3+}	Ce^{4+}	Ce^{3+}	Ce^{4+}	$P4_1$	$P2_1$
Ce1	Ce81	0.03	0.01	22.30	20.47	3.45	3.09	4.22	3.77	**III**	**III/IV**
	Ce83	0.04			20.77			3.98	3.56		**III/IV**
Ce2	Ce82	0.06	0.05	20.69	22.13	4.08	3.65	3.62	3.24	**III/IV**	**III**
	Ce84	0.01			22.91			3.32	2.97		**III**
Ce3	Ce85	0.06	0.02	19.57	19.49	4.61	4.13	4.72	4.22	IV	IV
	Ce87	0.04			19.99			4.73	4.23		IV
Ce4	Ce86	0.04	0.01	19.85	19.93	4.58	4.10	4.49	4.02	IV	IV
	Ce88	0.04			19.39			4.66	4.17		IV
Ce5	Ce91	0.06	0.02	24.07	24.39	4.58	4.10	4.55	4.07	IV	IV
	Ce93	0.04			23.75			4.71	4.22		IV
Ce6	Ce92	0.05	0.01	24.26	24.33	4.48	4.01	4.50	4.02	IV	IV
	Ce94	0.04			23.82			4.60	4.11		IV

Lithium atoms were located from difference-Fourier maps in the last runs of the structure resolution and geometrical considerations. In spite of the relatively weak scattering power of the lithium atoms, in both cases the same types of lithium sites were found. The existence of two kinds of lithium was also confirmed by ^{7}Li MAS NMR experiment. Both *Li2* and *Li3* lithium cations are free to move in the opened channels network. *Li1* corresponds to lithium cations confined in the locked slabs. Large shifts are observed for lithium positions between tetragonal and monoclinic models and lithium sites in the monoclinic model are far from positions correlated by the pseudo tetragonal screw axis. Lithium ions play an important role in the lowering of symmetry, but conclusion about lithium positions should be taken with care because of the weak scattering power of these ions that leads to a great uncertainty on their positions. Nevertheless, the introduction of the lithium is accompanied by the partial reduction of the cerium, and results into a long-range ordering between Ce^{3+} and Ce^{4+}. As it has been aforementioned, this long-range ordering led to the loss of the four-fold screw axis. Powder neutron diffraction experiments should be performed to obtain more information about the role of lithium atoms.

Table 2. Comparison of F and Li positions between the average $P4_1$ model and the correct $P2_1$ one (transformed in the tetragonal symmetry). Atom labels used for the $P2_1$ model correspond to [1].

Atom label		Atomic shift (Å)		Atom label		Atomic shift (Å)		Atom label		Atomic shift (Å)	
$P4_1$	$P2_1$	$P4_1$-$P2_1$	$P2_1$-$P2_1$	$P4_1$	$P2_1$	$P4_1$-$P2_1$	$P2_1$-$P2_1$	$P4_1$	$P2_1$	$P4_1$-$P2_1$	$P2_1$-$P2_1$
F01	F14	0.12	0.03	*F11*	F08	0.24	0.03	*F21*	F34	0.04	0.03
	F16	0.13			F12	0.24			F36	0.06	
F02	F06	0.12	0.02	*F12*	F33	0.02	0.08	*F22*	F30	0.02	0.06
	F09	0.14			F43	0.09			F31	0.07	
F03	F22	0.01	0.02	*F13*	F18	0.06	0.07	*F23*	F28	0.02	0.06
	F23	0.03			F24	0.02			F32	0.04	
F04	F02	0.13	0.04	*F14*	F10	0.25	0.03	*F24*	F49	0.05	0.02
	F05	0.13			F11	0.25			F50	0.04	
F05	F01	0.11	0.04	*F15*	F26	0.03	0.04	*F25*	F15	0.14	0.11
	F03	0.14			F40	0.05			F25	0.07	
F06	F04	0.11	0.10	*F16*	F21	0.07	0.08				
	F19	0.04			F42	0.08					
F07	F35	0.25	0.38	*F17*	F45	0.31	0.32	*Li1*	Li01	0.62	1.02
	F37	0.33			F47	0.32			Li02	1.37	
F08	F44	0.30	0.32	*F18*	F17	0.15	0.12	*Li2*	Li03	0.99	0.15
	F48	0.32			F27	0.09			Li06	1.12	
F09	F29	0.04	0.05	*F19*	F38	0.37	0.04	*Li3*	Li04	1.76	1.68
	F41	0.04			F39	0.40			Li05	0.09	
F10	F20	0.31	0.35	*F20*	F07	0.37	0.06				
	F46	0.19			F13	0.41					

References

1. Renaudin, G., Mapemba, E., Dubois, M., El-Ghozzi, M., Avignant, D. & Černý, R., in preparation.
2. Sheldrick, G.M., *SHELXS97* Program for the Determination of Crystal Structures, 1997, University of Göttingen, Germany.
3. Sheldrick, G.M., *SHELXL97* Program for Crystal Structure Refinement, 1997, University of Göttingen, Germany.
4. Rodriguez-Carvajal, J., Program *FullProf.2k*, Version 2.20, Laboratoire Léon Brillouin (CEA-CNRS), Saclay, France.

Acknowledgments. The authors are very indebted to the staff of the Swiss-Norvegian Beam Line (BM1) at ESRF in Grenoble, for providing help and facilities in the synchrotron powder diffraction experiment.